RSC Advances

ROYAL SOCIETY OF CHEMISTRY

www.rsc.org/advances

Graphical Abstract

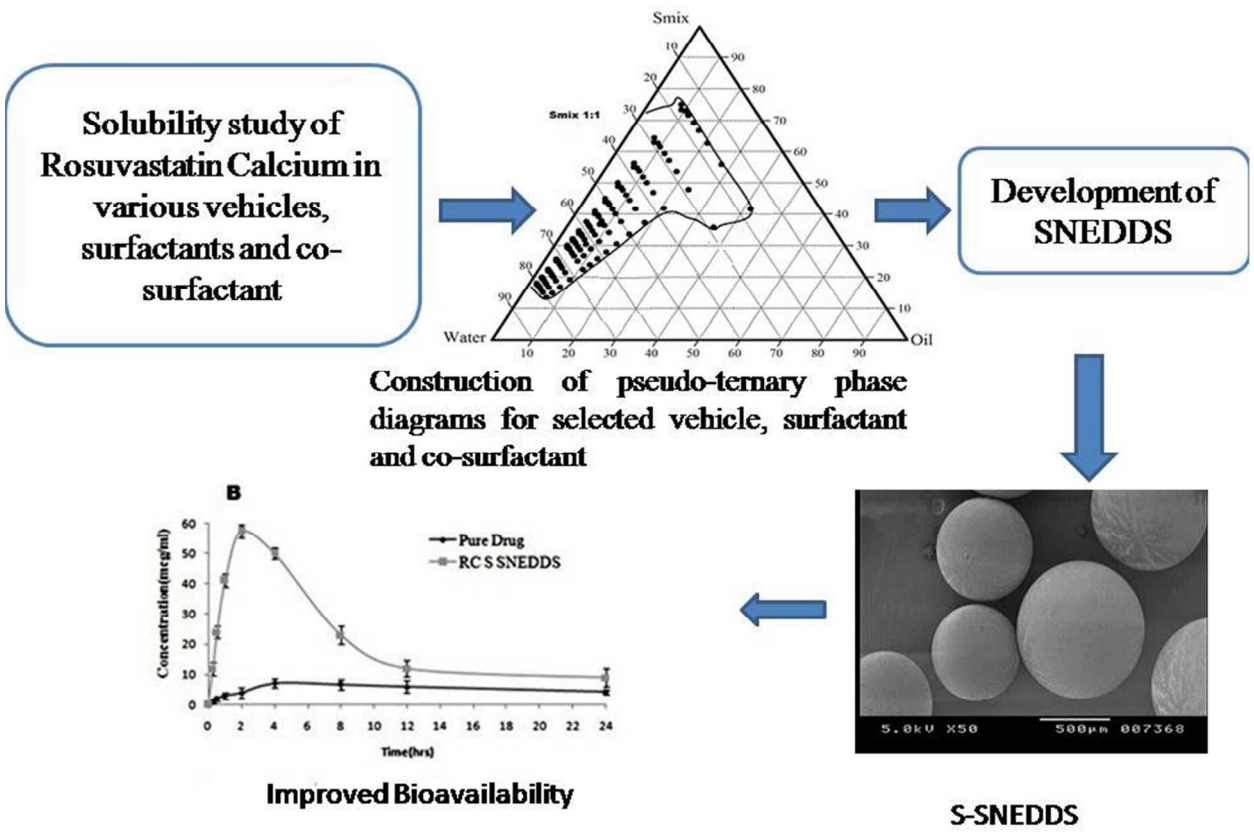

Porous Polystyrene Spheres Loaded Self Nano-emulsifying systems of Rosuvastatin calcium

Panner Selvam R[1*], Parthasarathi K Kulkarni[2], Naga Sravan Kumar Varma. V[2]

1. T John College of Pharmacy, Department of Pharmaceutics, Bangalore, Karnataka, India

2. JSS College of Pharmacy, Department of Pharmaceutics, JSS University,

Sri Shivarathreeshwara Nagar, Mysuru-570015, Karnataka, India

***Corresponding Author**:

Panner Selvam R

E-mail: selva.r9@gmail.com

Ph no: +91 9844795544

Abstract:

The aim of the study was to investigate potential of Solid Self Nano-emulsifying Drug Delivery System (SNEDDS) for enhancing solubility and oral bioavailability of Rosuvastatin Calcium (RC). RC solubility was determined in different vehicles such as oils, surfactants and co-surfactants. Capmul MCM (oil), tween 20 (surfactant) and PEG 200 were taken for the preparation of SNEDDS based upon the solubility of RC. Pseudo-ternary phase diagrams were constructed in order to identify efficient self-emulsifying regions. S-SNEDDS were prepared by adsorbing the optimized SNEDDS on to porous polystyrene spheres as a carrier. The S-SNEDDS formulated was free flowing and droplet size of the reconstituted nano-emulsion was almost unchanged after solidification. The prepared S-SNEDDS showed 98.92% release of RC at the end of 60 mins, whereas pure RC exhibited only 38.6%. The C_{max} and AUC_{0-t} of the S-SNEDDS was about 7.97 and 7.91 fold higher than the pure drug respectively. This research study gives an overview of the S -SNEDDS as a hopeful choice to improve the oral bioavailability of RC.

Keywords: S-SNEDDS; Rosuvastatin Calcium; SNEDDS; Pseudo-ternary phase diagrams; Porous polystyrene spheres; Solubility; oral bioavailability

Main Text

1. Introduction

Aqueous solubility and dissolution determines drug efficacy as well as its activity. In recent years, almost 70% of new drug candidates exhibit poor aqueous solubility[1]. Water insoluble drug can be delivered efficiently by crystal modifications, particle size reduction, complexation with cyclodextrins, pH modification, salt formation, solid dispersion, amorphization, emulsification using lipid carriers etc[2].

Self nano-emulsifying drug delivery systems (SNEDDS) are isotropic mixtures of lipids and surfactants, comprising of one or more hydrophilic co-solvents or co-emulsifiers which consists of drug that forms fine oil in water nano-emulsion upon mild agitation in an aqueous medium with droplet size ranging from 20-200 nm[3]. The significant advantages of SNEDDS include, depriving drug metabolism by cytochrome-P450 enzymes which are significantly present in the gut enterocytes and liver hepatocytes or by inhibiting P-glycoprotein efflux, bypassing the hepatic portal route and promoting lymphatic transport for lipophilic drugs[4]. SNEDDS have been a topic of interest to researchers in the recent past as these formulations have successfully improved oral bioavailability of poorly aqueous soluble drugs[5].

Usually SNEDDS are encapsulated into hard or soft gelatin capsules but due to its lipophilic nature, these formulations tend to interact with the capsule shell which causes brittleness or softness of the shell. Therefore, to overcome these drawbacks, liquid lipid formulations can be transformed to free flowing powders by loading them on a suitable carrier[6]. Such solid SNEDDS (S-SNEDDS) provides better stability, facility of manufacturing process, accuracy and improved patient compliance further adding to its advantage[7-10].

Hyperlipidemia is a heterogeneous disorder commonly characterized by increased flux of free fatty acids, increased triglyceride, LDL-cholesterol and apolipoprotein B levels, as well as decreased plasma HDL-cholesterol as a result of metabolic effects, dietary habits and life style[11]. Statins act by competitively inhibiting HMG-CoA reductase, which reduces the rate of production of the next mevalonate molecule that eventually produces cholesterol. This finally reduces cholesterol via several mechanisms[12]. Rosuvastatin bis [(E)-7-(4-(4-flurophenyl)-6-isopropyl-2-(methyl (methyl sulfonyl) amino) pyrmidin-5yl)(3R, 5S)-3,5-dihydroxyhept-6-enoic

acid)] calcium salt is a highly effective 3-hydroxyl-3-methylglutaryl coenzyme A (HMG CoA) reductase inhibitor[13]. Rosuvastatin calcium (RC) is crystalline in nature and has reduced aqueous solubility because of which the oral bioavailability is further reduced to 20%[14].

Balakumar *et al.,*[15] has successfully improvised solubility and bioavailability of RC using SNEDDS. In their study various oils including essential oils were evaluated with suitable surfactants and co-surfactants to prepared SNEDDS. However, current research is not only aimed towards improving solubility and oral bioavailability of RC by formulating the drug into SNEDDS, but also aimed to investigate the efficiency of porous polystyrene spheres (PPS) as a carrier for the prepared SNEDDS.

2. Materials and Methods

2.1. Materials

Rosuvastatin calcium (RC) was provided as a gift sample from Biocon, Bangalore, India**.** Labrafac PG, Labrafil M 1944 C S was obtained from Gattefosse, France (through Bombay College of Pharmacy, Mumbai, India). Capmul MCM, Captex 200 was provided by Abitec Group (USA). Porous polystyrene spheres (PPS) were provided as a gift sample from Thermax Limited, India. Spans 80, triethanolamine, PEG 800, PEG 200, oleic acid, castor oil were made commercially available from Merck, India. Tween 80, 20 and ethyla oleate were purchased from Loba Chemie pvt ltd, Mumbai, India. All the chemicals and buffers used were of analytical grade.

2.2. Solubility Study

Excess amount of RC was added to glass vials consisting 2 ml of selected vehicles (Table 1). Drug was mixed with oil manually for 30 mins, followed by sonication for 2 hrs. The mixture was then placed in water bath heated at 45ºC for 48 hrs in order to attain equilibrium followed by centrifugation at 3000 rpm for 20 mins. The drug dissolved was quantified spectrophotometrically at 243 nm.

2.3 FT-IR spectral analysis

The pure drug and physical mixtures (of selected oil, surfactant, co- surfactant, RC and PPS) were characterized for possible interactions through Fourier transform infrared (FT-IR) spectrometry. FT-IR spectral analysis was carried out by employing KBr press, followed by analyzing the prepared pellets using Fourier - Transform Infrared spectrometer, Shimadzu, Model 8033[16].

2.4 Construction of Pseudo-Ternary Phase Diagrams

Based upon RC solubility, suitable oil, surfactant and co-surfactant were selected and phase diagrams were sketched using Chemix software, considering different ratio of oil and surfactant:co-surfactent (S_{mix}). The ternary phase diagrams were developed by water titration method and the extent of nano-emulsion region (NE) was identified and established its relation to other phases[17]. Different ratios of mixture of oil: S_{mix} (1:0 (A), 1:1 (B), 1:2 (C), 1:3 (D), 1:4 (E), 2:1 (F), 3:1 (G) and 4:1 (H) wt/wt respectively) were diluted with water in a drop-wise manner. Samples were vortexed for 5min in order to apply same agitation for all the formulations.

2.5 Selection of Formulations

From the NE region of each constructed phase diagram, different concentrations of oil containing 10mg of RC, were selected with increments of 5% i.e. 10%, 15%, 20%, upto 40%. The composition utilizing minimal concentration of S_{mix} determined at every 5% oil increment was selected for its NE formulation.

2.6 Physiochemical Characterizations

2.6.1 Thermodynamic Stability Tests:

Different thermodynamic stability studies were carried out for selected formulations from phase diagram, in order to select metastable formulation[18]. The following studies were carried out with a minimal quantity of 3 ml and in replica of 3.

2.6.1.1 Centrifugation:

The SNEDDS formulations were subjected to centrifugal forces at 3500 rpm for 30 mins and checked for stability. The qualified formulations were subjected for heating and cooling cycle.

2.6.1.2 Heating and Cooling cycle (H/C cycle)

Temperature dependent stability of prepared NE was studied by H/C cycle. Six cycles at two different temperatures (4ºC and 45ºC) was carried out with storage at each of the temperature being not less than 48 hrs. The stable SNEDDS formulations were further subjected to freeze thaw cycle.

2.6.1.3 Freeze Thaw Cycle

Three free thaw cycles at -21ºC and +25ºC was carried out by storing the SNEDDS formulation for not less than 48 hrs at each followed by assessing of stability.

For all the above mentioned studies, the stability is assessed based on phase separation, creaming and cracking. The formulations that pass thermodynamic tests were taken for further studies.

2.6.2 Self-emulsification test

Selected SNEDDS formulations from the thermodynamic tests were subjected to self-emulsification/dispensability efficiency[18]. 0.5 ml of each selected formulations were dispersed in 500 ml of distilled water. Standard USP XXII dissolution apparatus type II was operated at 37ºC±0.5 and 50 rpm paddle speed. The formulations were visually examined and graded using following grade system:

Grade A: Rapidly formed NE (within 1 min), having a clear or bluish appearance.

Grade B: Rapidly formed NE (within 1 min), but slightly less clear or bluish white appearance.

Grade C: Fine milky emulsion formed within 2min.

Grade D: Dull, grayish white emulsion having slightly oily appearance that is slow to emulsify (longer than 2 min).

Grade E: either poor or minimal emulsification with large oil globules.

2.6.3 Robustness to Dilution

The selected SNEDDS formulations were studied for robustness upon dilution by diluting to 50, 100 and 1000 times in water and 0.1M HCl, followed by storage for 12 hrs in order to observe any signs of phase separation or drug precipitation.

2.6.4 Globule Size Determination and Polydispersity Index

Mean globule size and polydispersity index (PDI) were determined by monitoring light scattering at 25ºC at 90º angle using a Zetasizer 3000 (Malvern Instruments Worcestershire, UK)[19].

2.6.5 Viscosity

Viscosity was determined at 25ºC± 1.0º using Viscosity Brookfield DV III ultra V6.0 RV cone and plate rheometer (Brookfield Engineering Laboratories, INC., Middleboro, MA and spindle #CPE40). Rheocalc V2.6 was used for the calculations[20].

2.7 Preparation of Solid Self Nano-emulsifying Systems (S-SNEDDS)

Optimized SNEDDS formulation (0.5 ml containing 10mg of RC) was diluted with 2.0 ml ethanol in a stopper test tube followed addition of 400 mg of Porous Polystyrene spheres (PPS). This mixture was vortexed for 10 mins under ambient conditions. At 60ºC, ethanol evaporates with intermittent stirring and further, solid SNEDDS (S-SNEDDS) loaded PPS fractions were dried at 70ºC in an oven for about 2 hrs[21].

2.7.1 Characterization

RC and prepared S-SNEDDS were subjected to FTIR spectral analysis, Thermal Analysis and X-Ray Diffraction using Shimadzu, DSC 60 and X'Pert PRO diffractometer (PAN analytical, Netherlands) respectively[22]. FTIR spectral analysis was carried-out as mentioned in section 2.3.

2.7.2 Micromeritic properties

The prepared S-SNEDDS were studied for different micromeritic properties such as bulk density (ρ_b), tapped density (ρ_t), compressibility index, Hausner ratio and angle of repose (θ)[23]. A total quantity of 10gms of S-SNEDDS was taken as test sample.

Bulk density (ρ_b) is the ratio of total mass (M) of S-SNEDDS to the bulk volume (V_b) of S-SNEDDS. Tapped density (ρ_t) is the ratio of the mass (M) of the powder to the final tapped volume (V_t). Accurately weighed quantity of S-SNEDDS was carefully placed into the graduated cylinder through a funnel, and was tapped until there was no further reduction in volume. Compressibility index and the Hausner ratio were determined by measuring both the bulk volume and the tapped volume of a S-SNEDDS. The compressibility index (C) and Hausner ratio (H) may be calculated using measured values for bulk density (ρ_b) and tapped density (ρ_t) as following (equation 1 and 2):

$$\%C = \frac{\rho t - \rho b}{\rho t} X100 \quad \text{.....1}$$

$$H = \rho t / \rho b \quad \text{.....2}$$

Angle of repose is the maximum angle possible between the surface of a pile of the S-SNEDDS and the horizontal plane. Fixed funnel method was employed. The angle of repose (θ) was calculated using the given formula (equation 3):

$\tan(\theta)$ = Height/Radius…….3

2.7.3 Reconstitution Properties of S-SNEDDS

Hundred micrograms of S-SNEDDS were vortexed in 10 ml of distilled water for about 30 secs and incubated for 30 mins at 27±5ºC[24]. Further, reconstitution of S-SNEDDS was also performed in 10ml of 0.1 M HCL at 37ºC. The samples were vortexed only to ensure same agitation forces are applied for all the formulations. The average droplet size and PDI of NE from S-SNEDDS were determined using Zetasizer 3000 (Malvern instruments Worcestershire, U.K.) as mentioned in section 2.6.4.

2.7.4 Surface Morphology

The surface morphology of S-SNEDDS was examined using scanning electron microscope (Hitachi S3400, Tokyo, Japan).

2.7.5 Loading Efficiency

The ability of PPS to hold SNEDDS was determined using following equation 4[21].

$$\%\ loading\ efficiency = \frac{WL - WI}{WI} X100 \quad \ldots\ldots\ldots 4$$

Where WL is the weight of RC loaded S-SNEDDS, and WI is the initial weight of PPS**.**

2.7.6 Drug Content and drug loading

Theoretical yield of 10 mg equivalent RC loaded S-SNEDDS were extracted using methanol and analyzed for drug content using UV spectrophotometer at 243 nm. Drug content and drug loading were calculated using following equation 5 and 6.

$$Drug content = \frac{\text{Conc from standard graph x dilution factor}}{1000} \quad \text{----------5}$$

$$Drug Loading\% = \frac{\text{Practical Drug content}}{\text{theoretical drug content}} x100$$

2.7.7 *In Vitro* drug release studies

Drug release studies for 10mg pure RC and prepared S-SNEDDS (10mg equivalent weight) was determined in 900 ml of 0.1M HCl using USP dissolution type II apparatus at 37ºC±5º at 50 rpm. Aliquots were collected at predetermined time and quantified for drug release at 243 nm spectrophotometrically and replaced by same to maintain sink condition[4].

2.7.8 Oral pharmacokinetics

In vivo study approval was granted by the Institutional Animal Ethics Committee (Regd. No 107/2012). The experiments were directed as per the CPCSEA guidelines. Three groups of Wistar rats each consisting of six, irrespective of sex, weighing about 200-250 g, were housed under standard laboratory conditions as per the guidelines. The first group received distilled water, which acted as a control group, and the other two groups were administered with a

suspension of pure and RC loaded S-SNEDDS (10 mg equivalent weight of RC). Prior to administration, rats were subjected to overnight fasting with a provision of drinking water. Oral dosage was calculated w.r.t. surface area ratio of rat to that of human. Blood samples were collected from the tail vein at predetermined time after administration. Separation of plasma from blood was achieved by centrifugation of blood samples at 1000 rpm for 10 mins.

Plasma drug concentration (PDC) was determined by a validated HPLC method. The drug was extracted from plasma by adding 1.0 ml of diethyl ether followed by vortexing and centrifuging for 5 min at 3500 rpm at 0ºC respectively. Organic layer was separated and evaporated for complete dryness using gentle stream of nitrogen on a heating block maintained at 40ºC. The residue obtained was reconstituted using Methanol-Water (68:32 v/v; pH adjusted to 3.0 with trifluoroacetic acid) as a mobile phase. The samples were injected into C18 column at a flow rate of 1.5 ml/min and quantified at 243nm. Pharmacokinetics parameters such as C_{max}, T_{max}, $t_{1/2}$, K_a and AUC_{0-t} were determined from plasma concentration time-profile[4, 25].

2.7.8 Stability study

Formulated RC S-SNEDDS stability was determined at 40ºC/75%RH for 3 months. At an interval of 0, 1, 2 and 3 months the samples were withdrawn and analyzed for physical, chemical stability, drug content and *in vitro* drug release.

3. Results and Discussion

3.1 Solubility studies

Drug solubility in selected oils, surfactants and co-surfactants was evaluated and the results are depicted in Table 1. Excipients that could solubilize and obtain highest drug concentration level, for the preparation of SNEDDS, were selected in order to facilitate loading on or within solid matrices[18]. Because of low solubility of the drug, stability and biocompatibility issues, the natural lipids were not selected for formulation. Amongst the selected excipients, RC exhibited highest solubility in capmul MCM (oil), tween 20 (surfactant) and PEG 200 (Co surfactant). Capmul MCM comprises a mixture of C8/C10 mono-/diglycerides which completely solubilizes the drug in the vicinity of triglyceride chains that could be attributed to a shorter chain length [26]. Tween 20, a non-ionic surfactant with a high hydrophilic-lipophilic balance

(HLB), was screened for high solubility as well as safety concerns. It has been reported, that use of co-surfactants along with surfactants helps in reduction of surface tension by assembling at the interfacial layer and also it tends to fluidize the interfacial surfactant film, thereby improving the area of nano-emulsion region[27]. Hence PEG 200 was selected for our present research as a co-surfactant.

Table 1: Solubility of RC in various excipients

Excipients	Solubility(mg/ml)*
Ethyl Oleate	15±1.2
PG	320.2±4.3
PEG200	367±6.2
PEG 400	352.3±3.8
Oleic acid	12±1.5
Tween 80	28±2.1
Tween 20	184.1±3.7
Capmul MCM	127±1.1
Captex 200	17.2±1.5
Labrafil	32±2.9
Labrafac	16±1.6
Labrasol	153.9±3.7
Capryol 90	42±1.8
Castor oil	12±1.3
Span 20	26.4±1.9
Span 80	28.1±2.1
Isopropyl myristate	19±1.5
Palm oil	5.7±1.1
Sunflower oil	8.2±1.8

(*Mean±SD, n=3)

3. 2 FT-IR spectra

The FTIR spectra observed for RC, SNEDDS and S-SNEDDS were sketched and compared in fig. 1 whereas, FTIR spectra for all the physical mixtures were presented in supplemental data sheet. Pure RC displays characteristic peaks at 3379.40 cm^{-1}, 2970.48 cm^{-1}, and 1720.56 cm^{-1} corresponding to O-H stretching, N-H stretching and C=O stretching of acid respectively. The other principal peaks are observed at 1550.82 cm^{-1} for C=C stretching, 2931.90 cm^{-1} for =C-H stretching, 1442.80 cm^{-1} and 1381.08 cm^{-1} for asymmetric and symmetric bending vibration of CH_3 group respectively, 1327.07 cm^{-1} for asymmetric vibration of S=O, 779.27 cm^{-1}, 570.95 cm^{-1} and 516.94 cm^{-1} corresponds to absorption bands of out of plane for

C=C of benzene ring and 1226.77 cm^{-1} for bending vibration for C-H. The FTIR spectral data of RC when compared to physical mixtures, SNEDDS and S-SNEDDS has shown shift in intensity of the absorption bands. The shift observed for 2970.48 cm^{-1} and 1720.56 cm^{-1} peaks might be due to lower and higher frequency stretching vibrations of N-H and C=O respectively. However, no drug interaction was observed, confirming RC is compatible with all the ingredients used.

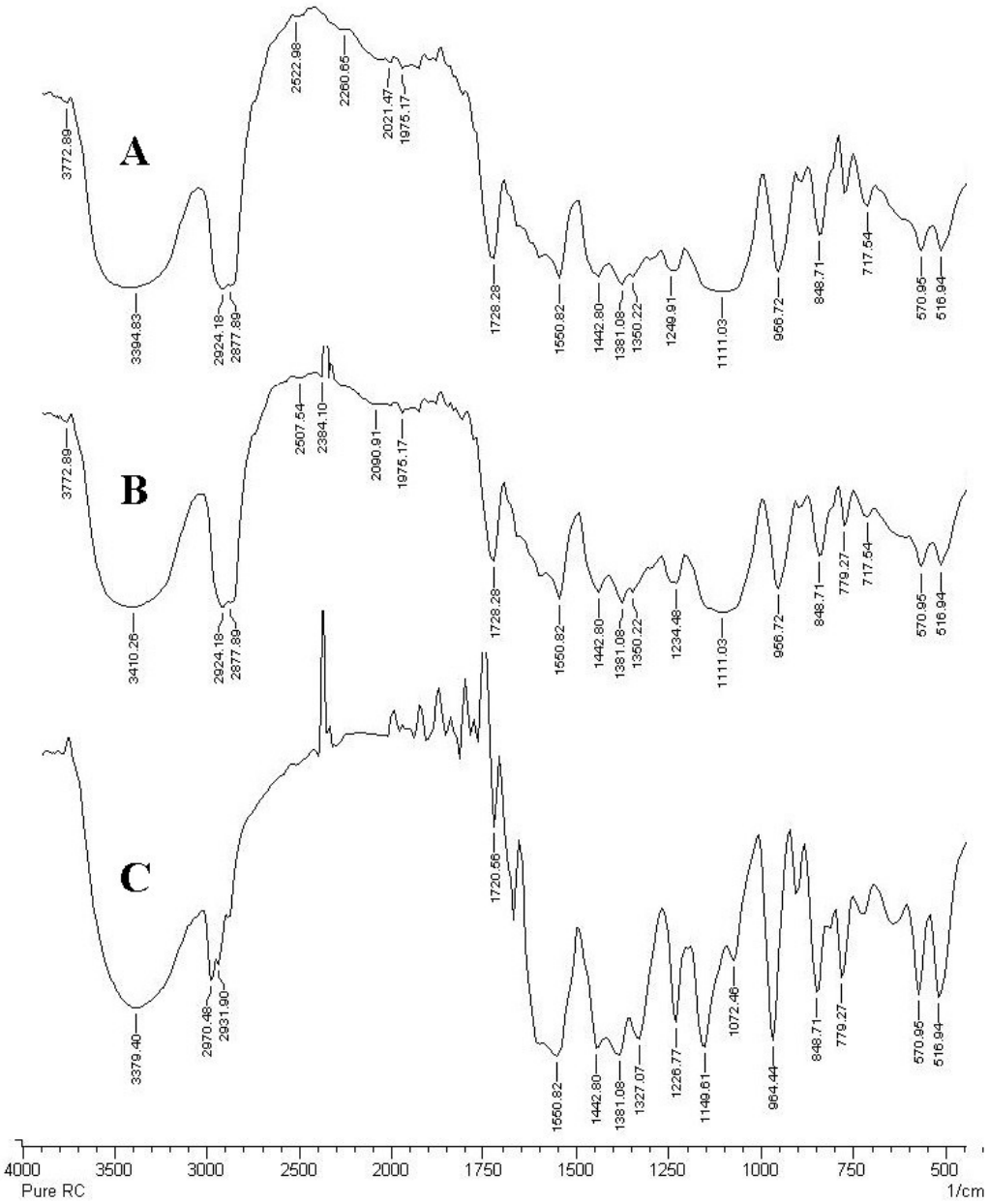

Fig. 1. IR spectra of A) S-SNEDDS, B) SNEDDS and C) pure RC.

3.3 Construction of Pseudo Ternary Phase Diagram

Pseudo ternary phase diagrams were constructed in order to identify self nano-emulsifying regions as well as to determine the concentration of oil, surfactant and co-surfactant and to develop stable RC loaded SNEDDS. A constructed phase diagram of oil-S_{mix}-water system (S_{mix} 1:1) is depicted in Fig.2. To avoid over-crowding, phase diagram was simplified to exclusively exhibit nano-emulsion region. The Pseudo ternary phase diagrams of different ratios of mixture of oil: S_{mix} (1:0, 1:1, 1:2, 1:3, 1:4, 2:1, 3:1 and 4:1 wt/wt respectively) were further reported in supplemental data sheet.

In our preliminary review and findings (not shown here), high HLB value of an emulgent facilitates lowering of interfacial energy, which in turn, forms a stable nano-emulsion. Selected excipients have high HLB values and synergistic effect of excipients reduces interfacial tension as well as nano-emulsion formation[28].

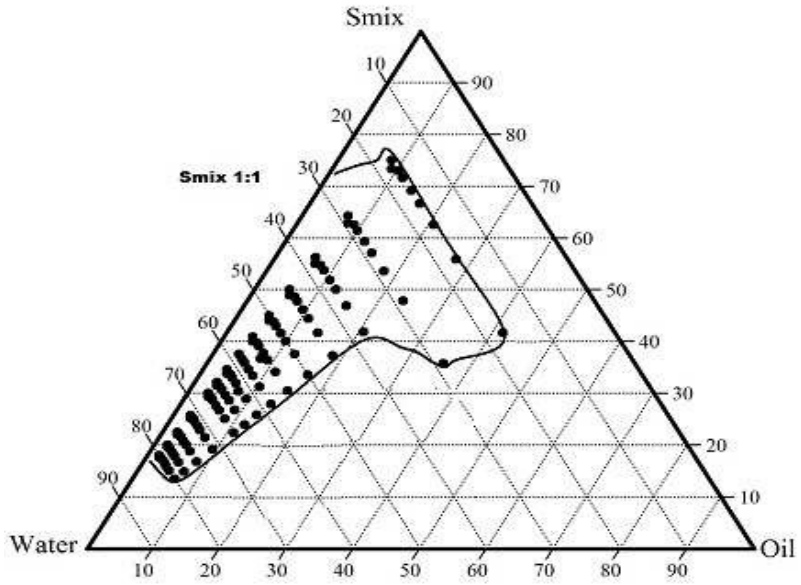

Fig. 2.Pseudoternary phase diagram of system with the following components: Capmul MCM (oil), Tween 20(surfactant), PEG 200(Cosurfactant).

3. 4 Selection of Formulations from Phase Diagrams

Constructed phase diagrams depicts that oil could be solubilized at an extent of 42% w/w. Hence, different concentrations of oil at selected 5% w/w increment (10%, 20%, 25%, 30%, 35%, 40% w/w), was utilized for preparation of nano-emulsion. This allows selection of various formulations covering the entire nano-emulsion area of phase diagram.

To avoid or avert surfactant related risk of hemolysis and gastric disturbances, the concentration was kept at minimum possible level. Out of all the prepared formulations, B20, D20, F25, F30 and G30 (Table 2) were stable at a wide range of temperatures and centrifugal stress without any oil-water separation, agglomeration and precipitation of drug (observations of thermodynamic stability test are presented in supplemental data sheet). The thermodynamic stability of selected formulation might be due to adsorption of surfactant/co-surfactant at the interface that decreases the interfacial energy which is required for zeroing coalescence[29]. The optimized SNEDDS emulsifies within a minute, giving bluish appearance nano-emulsion. The prepared SNEDDS did not show any sign of drug precipitation after diluting it with larger amount of dissolution media.

Table 2: Optimized formulations selected from phase diagram at a difference of 5% w/w of oil that passed thermodynamic stability test and dispersion test with its particle size, PDI and viscosity

Formulation Code	Smix ratio	Oil %	Surfactant %	Co-Surfactant %	Aqueous %	Particle Size (nm)	PDI	Viscosity (cps)*
B20	1:1	20	20	20	40	35.27	0.127	20.4±0.6
D20	1:3	20	14	42	24	44.83	0.198	22.5±0.8
F25	2:1	25	14.6	7.3	53	68.16	0.242	23.1±0.5
F30	2:1	30	18.6	9.3	42	123.49	0.341	27.8±0.3
G30	3:1	30	21.7	7.3	41	97.68	0.296	28.6±0.2

(*Mean±SD, n=3).

3.5 Particle Size

The particle sizes of the prepared SNEDDS were in the following order B20<D20<F25<G30<F30. Out of the 5 formulations, B20 shows smaller particle size of

35.27 nm (Fig. 3. (A)) and poly dispersibility index (PDI) value was low (0.127) indicating narrow size distribution. This small particle size could be attributed to high concentration of surfactant and low concentration of oil. Beyond oil concentration of 42% w/w, micro emulsions are formed. The increase in particle size might be attributed due to lack of emulsification of oil in absence of surfactant/co surfactant. Nature of type of oil employed has a significant effect on the droplet size of the emulsion as it has been reported previously. In-proportionate invasion, into surfactant alkyl chain region, by oil molecules influences interfacial film composition as well as its flexibility. An alteration in interfacial film has a direct effect on the droplet surface curvature thereby causing differences in globule size[30].

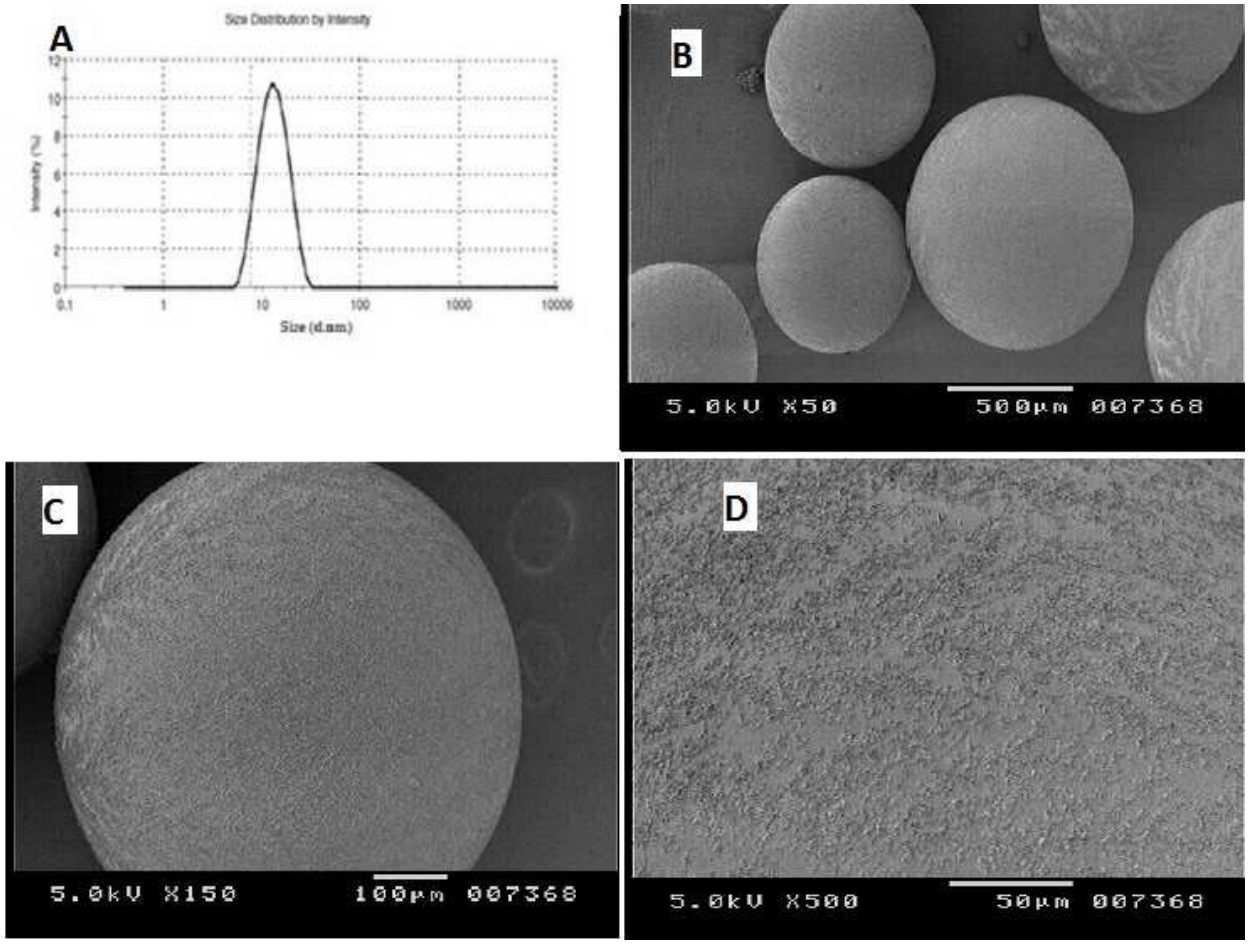

Fig. 3.Particle size distribution of SNEDDS (A) and Scanning electron micrographs of Porous Polystyrene Spheres loaded SNEDDS (S-SNEDDS) at different magnification (B-D).

3.6 Viscosity

The viscosities of all formulations were in nearby range (Table 2), revealing Newtonian type of flow characteristics. It is observed that the viscosity of the formulation is directly proportional to viscosity of oil and surfactant. As suggested in previous reports, SNEDDS with lower viscosity tend to form o/w type of nano-emulsion system and exhibit Newtonian type of flow behavior[31]. Based on the evaluation results, formulation B20 was considered as optimized and was chosen for solidification.

3.7 Preparation of Solid Self Nano-emulsifying Systems (S-SNEDDS)

In order to improve the acceptance, prepared liquid SNEDDS were loaded onto PPS by adsorption method to formulate into S-SNEDDS. The ideal solid matrix excipients for preparation of S-SNEDDS should have high adsorption capacity, which could hold a larger liquid SNEDDS[32]. PPS is a robust, polymeric adsorbent synthesized from cross-linked polystyrene having no ionic functional group having high specific surface area 550 m^2/g (BET) and porosity (0.4 ml/ml of bead). The RC loaded S-SNEDDS in this study were prepared by loading 0.5 ml of B20 containing 10mg of RC over 400 mg of PPS, as described in section 2.7.

Micromeritic properties of prepared RC loaded S-SNEDDS are listed in Table no.3. The bulk density was found to be 0.6g/ml, as the PPS were spherical in shape, which takes less surface for filling. The Angle of repose, Hausner ratio and percentage compressibility indicate the prepared formulations show good flow properties. Loading efficiency indicates the ability of PPS to hold SNEDDS. The loading efficiency of PPS was high (i.e., 112.7) due to increased pores and surface area available for adsorption.

Table 3: Evaluation parameters of RC loaded S-SNEDDS formulations.

Parameters	Value*
Loose bulk density g/cc	0.561±0.023
Tapped bulk density g/cc	0.6±0.08
Percent compressibility	6.5±1.1

Hausner ratio	1.069±0.043
Angle of repose	23.02±2.2
Loading efficiency (%)	112.7±4.7
Size of the globule (nm) in water at 27º	37.6
PDI in water at 27º	0.148
Size of the globule (nm) in 0.1 M HCL at 37ºC	36.5
PDI in 0.1 M HCL at 37ºC	0.163

(*Mean±SD, n=3).

3.8 Reconstitution Properties of Solid SNEDDS

Reconstitution properties were determined by introducing prepared S-SNEDDS into aqueous phase and 0.1 M HCL which forms o/w emulsion by vortexed. The z-average, particle diameter and PDI of S-SNEDDS are presented in Table no.3. When compared to SNEDDS (results depicted in section 3.5 and table 2), no significant change in the mean droplet size of RC loaded S-SNEDDS was observed indicating no interruption of formation of nano-emulsion upon dilution.

3.9 Surface morphology

Surface morphology of S-SNEDDS was given in Fig.3 (B-D). The SEM images reveal that S-SNEDDS appeared to be separated, uniform and spherical in shape. The average particle size of S-SNEDDS was found to be 652±12µm. SEM images reveal that PPS has porous surface with high surface area that enables it to be used as an efficient carrier for lipid loading. Absence of drug crystals in S-SNEDDS image confirms complete incorporation of SNEDDS in the PPS matrix system.

3.10 Differential Scanning Calorimetry studies

DSC thermographs of RC and prepared S-SNEDDS are given in Fig.4. The thermographs reveal endothermic melting peak at 128 ºC, corresponding with its melting point and crystalline nature. The absence of drug peak in formulated S-SNEDDS might be due to molecular dispersion of the drug in lipid excipients[7].

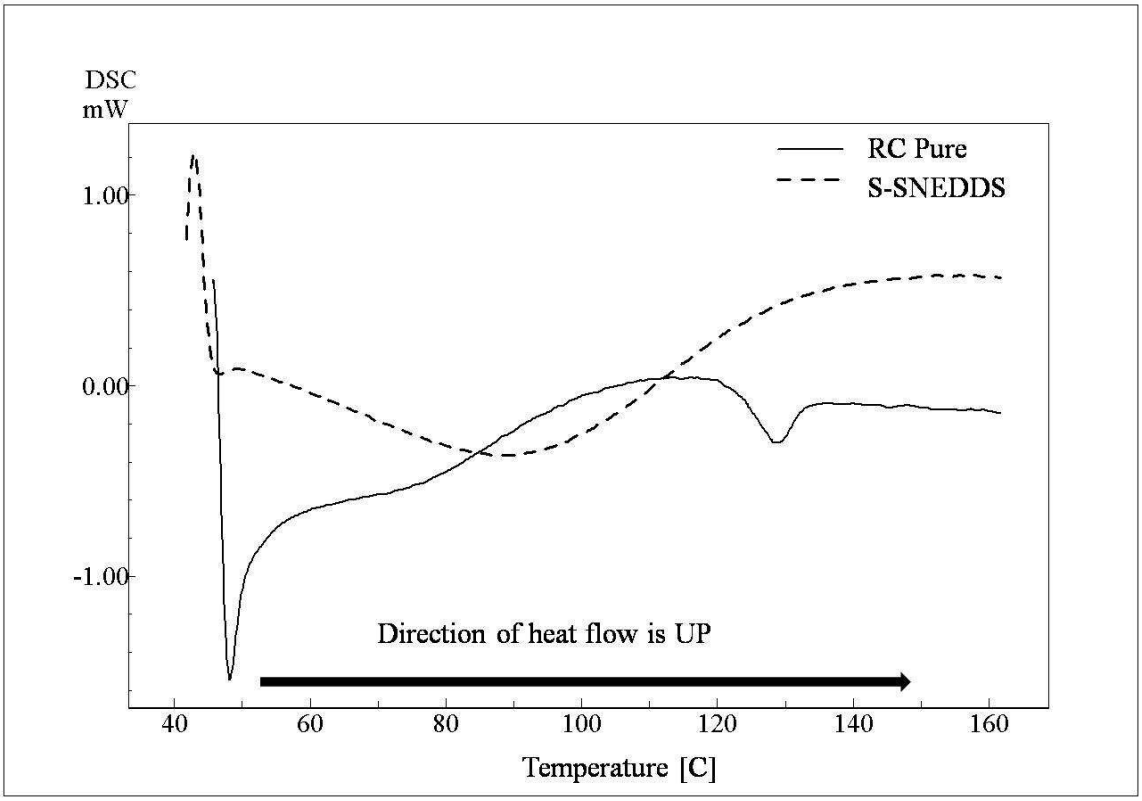

Fig. 4. DSC thermographs of RC pure and S-SNEDDS

3.11 X-Ray Diffraction studies

The spectra of X-ray diffraction study are presented in Fig. 5. Sharp high intensity peaks of pure RC exhibits its characteristic crystalline pattern. Whereas in case of prepared RC S-SNEDDS, there were no apparent peaks defining crystals of RC observed. The outcome obtained by XRD spectra were supported by SEM images and DSC thermographs. This confirms that drug in S-SNEDDS is present in a solubilized state within the excipients[23].

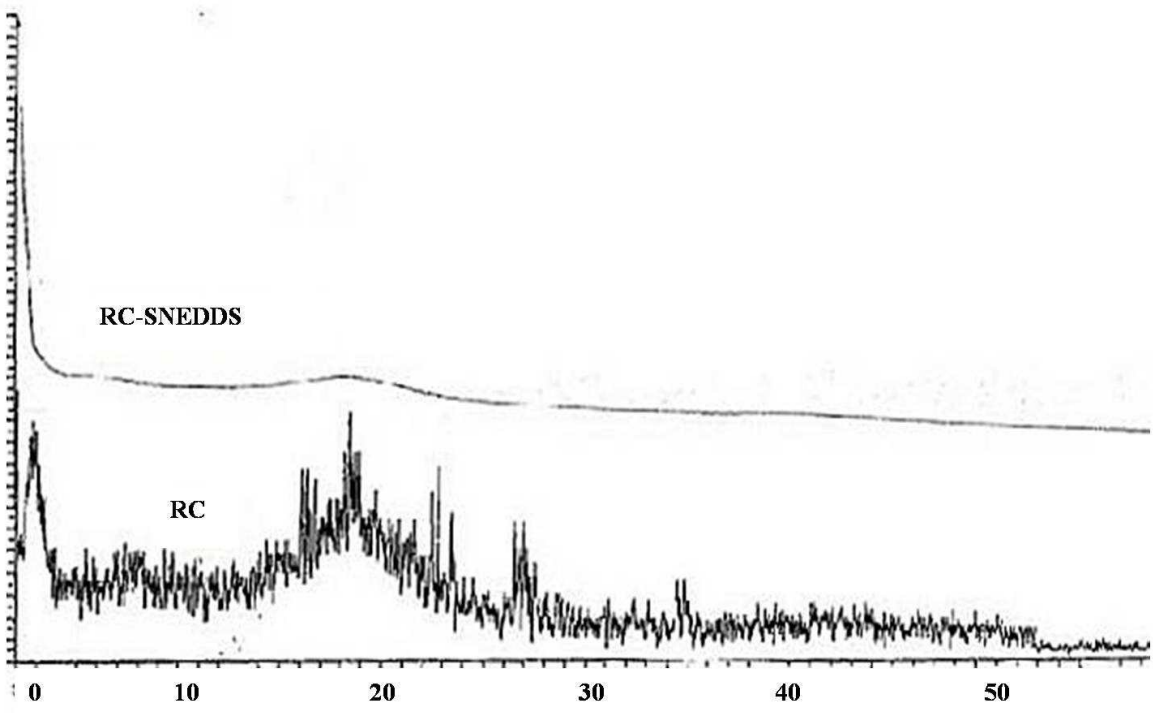

Fig. 5. XRD spectra pure drug and S-SNEDDS.

3.12 Drug Content and *In Vitro* drug release studies

Drug content in the prepared S-SNEDDS was found to be 1.10 % w/w (∴ each 100 mg of S-SNEDDS contain 1.10 mg of RC). When compared with theoretical drug content 99.2% of drug was found to be loaded (theoretically each 900 mg of S-SNEDDS contains 10mg of drug). The *in vitro* drug release from the prepared S-SNEDDS after initial 10min was found to be 42.2%. This initial burst release could be attributed to presence of drug on the surface of PPS matrix carrier[6]. According to the theory of thermodynamic formation of nano-emulsion, emulsification occurs when entropy change that favors dispersion, is greater than the energy required to increase the surface area of dispersion and free energy (ΔG) is negative[6, 33]. Alternative theory suggests ease of emulsification is dependent upon penetration of water into oil-water interface as well as generation of liquid crystalline phase resulting in swelling at the interface[26].

At the end of 60 min, prepared S-SNEDDS exhibited 98.92% drug release as compared to 38.6% of that of pure drug (Fig. 6). The small dimension of oil droplets provides large specific surface

area in direct contact with that of the dissolution medium or the molecular dispersed state of drug might be the underlying cause for better drug release.

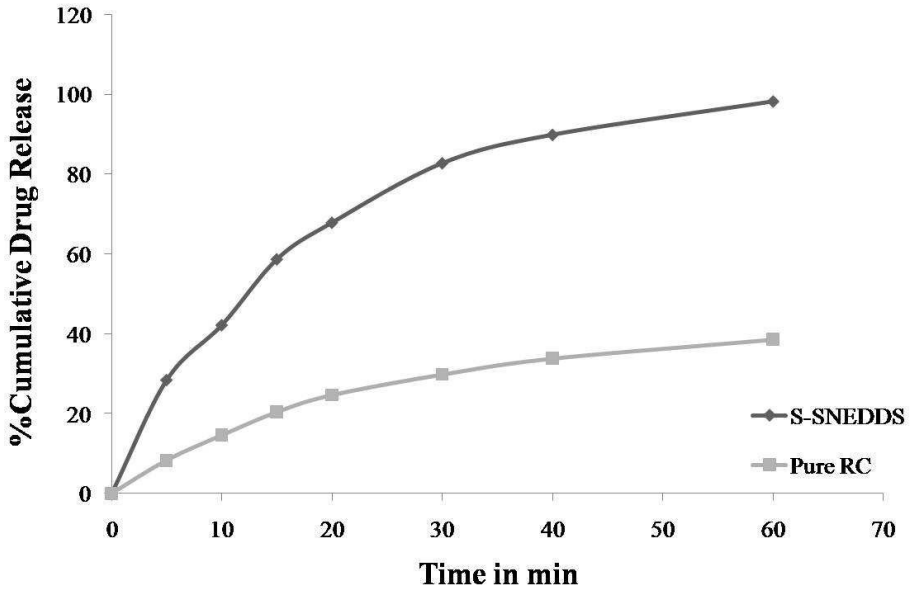

Figure 6: *In-vitro* % cumulative drug release of RC S-SNEDDS and pure RC

3.13 Oral pharmacokinetics

The Pharmacokinetic study indicates that the RC S-SNEDDS shows significant improvement of C_{max} and bioavailability of the drug when compared to its pure form (Fig. 5 and table 4). Nano-emulsified provide large interfacial area for enzyme pancreatic lipase to hydrolyse triglycerides thereby promoting faster and greater release of drug. This in turn enhances oral absorption and bioavailability[34].

As in Fig. 7; it can be observed that the C_{max} and AUC_{0-t} of S-SNEDDS was about 7.97 and 7.91 fold higher than pure drug respectively. The enhanced oral absorption of lipophilic drugs by the SNEDDS approach is because of enhanced dissolution rate of the drug in the aqueous media as well as increased tissue uptake. The solubilized drug is absorbed via paracellular or transcellular absorption. Other mechanisms may include diffusion of the solubilized drug as nano-emulsion droplets and absorption as bile acids mixed micelles[19]. Similarly, it is evident from the plasma concentration profiles that t_{max} decreases for S- SNEDDS (1.9 h) compared to the pure drug

(5 h). The obtained result signifies that the prepared S-SNEDDS have the improved bioavailability compared to the pure drug.

Table 4: Pharmacokinetic parameters for S-SNEDDS and pure RC

Product	C_{max} (mcg/ml)	T_{max} (h)	K_{el}	$T_{1/2}$	$(AUC)_0^t$
RC	7.2	5	0.04	16.4	52.9
RC S-SNEDDS	57.4	1.9	0.04	14.2	418.6

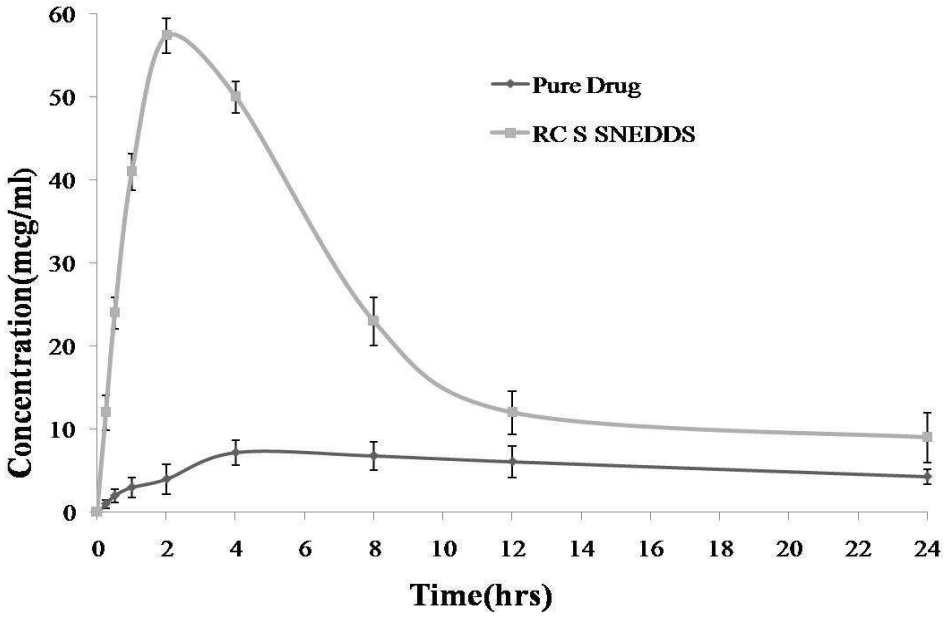

Fig. 7. *In vivo* drug release profile of pure drug and S-SNEDDS.

3.14 Stability Studies

The result of the stability studies of RC S-SNEDDS stored at 40°C and 75% relative humidity for 3 months showed no significant change in the appearance and drug content. The FT-IR spectral data and drug release behavior of the optimized formulation also remained unchanged. Hence, the prepared optimized formulation was found to be stable at 40°C and 75% RH (Table 4).

Table 4: Stability data study data of optimized formulation stored at at 40°C and 75% relative humidity.

Test interval	FTIR	Drug content (%)	%Cumulative drug release after 60 min
Initial	Complies	99.14±0.58	98.79±0.74
1 month	Complies	98.34±0.64	98.22±0.62
2 month	Complies	98.02±0.28	97.68±0.86
3 month	Complies	98.47±0.46	99.23±0.29

(*Mean±SD, n=3).

4. Conclusions

In our present research, potential of S-SNEDDS as a novel drug delivery system for RC was investigated. RC loaded SNEDDS was prepared using different concentrations of Capmul MCM, Tween 20 and PEG 200 of which, formulation B20 comprising of 20% oil, 20% surfactant and 20% co-surfactant was found to be optimized based upon the results obtained. In order to improve the acceptability, formulated B20 was further adsorbed onto porous polystyrene spheres to produce S-SNEDDS. The prepared S-SNEDDS exhibited good micromeritic properties as well preserving self-nano-emulsification properties of SNEDDS. S-SNEDDS significantly improved dissolution properties, oral bioavailability of RC when compared to that of pure drug. The result obtained provides a platform for formulating BCS class-II drugs successfully into S-SNEDDS for enhancing oral bioavailability.

5. Acknowledgements

The authors are duly indebted to Biocon, Bangalore, India for providing us with gift sample of Rosuvastatin Calcium. We would also like to show our gratitude to Gattefosse, France and Abitec group, USA for providing us with excipients sample.

6. References

1. Y. Kawabata, K. Wada, M. Nakatani, S. Yamada and S. Onoue, *International journal of pharmaceutics*, 2011, **420**, 1-10.
2. L. Wang, J. Dong, J. Chen, J. Eastoe and X. Li, *Journal of colloid and interface science*, 2009, **330**, 443-448.
3. A. M. Villar, B. C. Naveros, A. C. Campmany, M. A. Trenchs, C. B. Rocabert and L. H. Bellowa, *International journal of pharmaceutics*, 2012, **431**, 161-175.
4. B. Singh, R. Singh, S. Bandyopadhyay, R. Kapil and B. Garg, *Colloids and surfaces. B, Biointerfaces*, 2013, **101**, 465-474.
5. Z. Wang, J. Sun, Y. Wang, X. Liu, Y. Liu, Q. Fu, P. Meng and Z. He, *International journal of pharmaceutics*, 2010, **383**, 1-6.
6. V. Agarwal, A. Siddiqui, H. Ali and S. Nazzal, *International journal of pharmaceutics*, 2009, **366**, 44-52.
7. V. R. Kallakunta, S. Bandari, R. Jukanti and P. R. Veerareddy, *Powder Technology*, 2012, **221**, 375-382.
8. H. Zhou, J. Wan, L. Wu, T. Yi, W. Liu, H. Xu and X. Yang, *PloS one*, 2013, **8**, e84530.
9. B. K. Nanjwade, D. J. Patel, R. A. Udhani and F. V. Manvi, *Sci Pharm*, 2011, **79**, 705-727.
10. S. Gupta, R. Kesarla and A. Omri, *ISRN Pharm*, 2013, **2013**, 848043.
11. G. D. Kolovou, K. K. Anagnostopoulou and D. V. Cokkinos, *Postgraduate medical journal*, 2005, **81**, 358-366.
12. J. W. Cheng, *Clinical therapeutics*, 2004, **26**, 1368-1387.
13. Y. Mori, G. Kuriyama, T. Tanaka and N. Tajima, *Endocrine*, 2009, **36**, 412-418.
14. M. Schachter, *Fundamental & clinical pharmacology*, 2005, **19**, 117-125.
15. K. Balakumar, C. V. Raghavan, N. T. selvan, R. H. prasad and S. Abdu, *Colloids and surfaces. B, Biointerfaces*, 2013, **112**, 337-343.
16. S. Beg, S. S. Jena, N. Patra Ch, M. Rizwan, S. Swain, J. Sruti, M. E. Rao and B. Singh, *Colloids and surfaces. B, Biointerfaces*, 2013, **101**, 414-423.
17. S. Shafiq-un-Nabi, F. Shakeel, S. Talegaonkar, J. Ali, S. Baboota, A. Ahuja, R. K. Khar and M. Ali, *AAPS PharmSciTech*, 2007, **8**, Article 28.
18. N. Subramanian, S. Ray, S. K. Ghosal, R. Bhadra and S. P. Moulik, *Biological & pharmaceutical bulletin*, 2004, **27**, 1993-1999.
19. E. Atef and A. A. Belmonte, *European journal of pharmaceutical sciences : official journal of the European Federation for Pharmaceutical Sciences*, 2008, **35**, 257-263.
20. M. Gulam, I. K. Zeenat, B. Tripta and T. Sushama, *Current Nanoscience*, 2009, **5**, 428-440.
21. P. Patil and A. Paradkar, *AAPS PharmSciTech*, 2006, **7**, E28.
22. S. Shanmugam, R. Baskaran, P. Balakrishnan, P. Thapa, C. S. Yong and B. K. Yoo, *European journal of pharmaceutics and biopharmaceutics : official journal of Arbeitsgemeinschaft fur Pharmazeutische Verfahrenstechnik e.V*, 2011, **79**, 250-257.
23. R. P. Dixit and M. S. Nagarsenker, *European journal of pharmaceutical sciences : official journal of the European Federation for Pharmaceutical Sciences*, 2008, **35**, 183-192.

24. T. Yi, J. Wan, H. Xu and X. Yang, *European journal of pharmaceutics and biopharmaceutics : official journal of Arbeitsgemeinschaft fur Pharmazeutische Verfahrenstechnik e.V*, 2008, **70**, 439-444.
25. J. Zhang, Y. Gao, S. Qian, X. Liu and H. Zu, *International journal of pharmaceutics*, 2011, **414**, 186-192.
26. S. R. Panner, P. K. Kulkarni and D. Mudit, *Indian Journal of Pharmaceutical Education and Research*, 2013, **47**, 47-54.
27. R. S. Kalhapure and K. G. Akamanchi, *International journal of pharmaceutics*, 2012, **425**, 9-18.
28. A. Mullertz, A. Ogbonna, S. Ren and T. Rades, *The Journal of pharmacy and pharmacology*, 2010, **62**, 1622-1636.
29. S. V. Rao and J. Shao, *International journal of pharmaceutics*, 2008, **362**, 2-9.
30. L. Wei, P. Sun, S. Nie and W. Pan, *Drug development and industrial pharmacy*, 2005, **31**, 785-794.
31. A. Niederquell, A. C. Volker and M. Kuentz, *International journal of pharmaceutics*, 2012, **426**, 144-152.
32. P. Balakrishnan, B.-J. Lee, D. H. Oh, J. O. Kim, M. J. Hong, J.-P. Jee, J. A. Kim, B. K. Yoo, J. S. Woo, C. S. Yong and H.-G. Choi, *European Journal of Pharmaceutics and Biopharmaceutics*, 2009, **72**, 539-545.
33. M. Noriyuki, K. Mariko, N. Yasuko, M. Shozo and S. Hitoshi, *International journal of pharmaceutics*, 1980, **4**, 271-279.
34. T. Iosio, D. Voinovich, B. Perissutti, F. Serdoz, D. Hasa, I. Grabnar, S. D. Acqua, G. P. Zara, E. Muntoni and J. F. Pinto, *Phytomedicine : international journal of phytotherapy and phytopharmacology*, 2011, **18**, 505-512.